



Published in final edited form as:

Cell Rep. 2016 September 6; 16(10): 2723–2735. doi:10.1016/j.celrep.2016.08.002.

NGF-TrkA signaling by sensory nerves coordinates the vascularization and ossification of developing endochondral bone

Ryan E. Tomlinson¹, Zhi Li¹, Qian Zhang¹, Brian C. Goh¹, Zhu Li¹, Daniel L. J. Thorek^{2,3}, Labchan Rajbhandari⁴, Thomas M. Brushart¹, Liliana Minichiello⁵, Fengquan Zhou¹, Arun Venkatesan⁴, and Thomas L. Clemens^{1,6}

¹Department of Orthopaedic Surgery, Johns Hopkins University, Baltimore, MD 21287, USA

²Department of Radiology and Radiological Sciences, Johns Hopkins University, Baltimore, MD 21287, USA

³Department of Oncology, Johns Hopkins University, Baltimore, MD 21287, USA

⁴Department of Neurology, Johns Hopkins University, Baltimore, MD 21287, USA

⁵Department of Pharmacology, Oxford University, Oxford, OX1 3QT, UK

⁶Baltimore Veterans Administration Medical Center, Baltimore, MD 21201, USA

SUMMARY

Developing tissues dictate the amount and type of innervation they require by secreting neurotrophins, which promote neuronal survival by activating distinct tyrosine kinase receptors. Here, we show that NGF-TrkA signaling directs innervation of the developing mouse femur to promote vascularization and osteoprogenitor lineage progression. At the start of primary ossification, TrkA positive axons were observed at perichondrial bone surfaces, coincident with NGF expression in cells adjacent to centers of incipient ossification. Inactivation of TrkA signaling during embryogenesis in TrkA^{F592A} mice impaired innervation, delayed vascular invasion of the primary and secondary ossification centers, decreased numbers of Osx-expressing osteoprogenitors, and decreased femoral length and volume. These same phenotypic abnormalities were observed in mice following tamoxifen-induced disruption of NGF in Col2-expressing perichondrial osteochondral progenitors. We conclude that NGF serves as a skeletal neurotrophin to promote sensory innervation of developing long bones, a process critical for normal primary and secondary ossification.

Correspondence: tclemens5@jhmi.edu.

Publisher's Disclaimer: This is a PDF file of an unedited manuscript that has been accepted for publication. As a service to our customers we are providing this early version of the manuscript. The manuscript will undergo copyediting, typesetting, and review of the resulting proof before it is published in its final citable form. Please note that during the production process errors may be discovered which could affect the content, and all legal disclaimers that apply to the journal pertain.

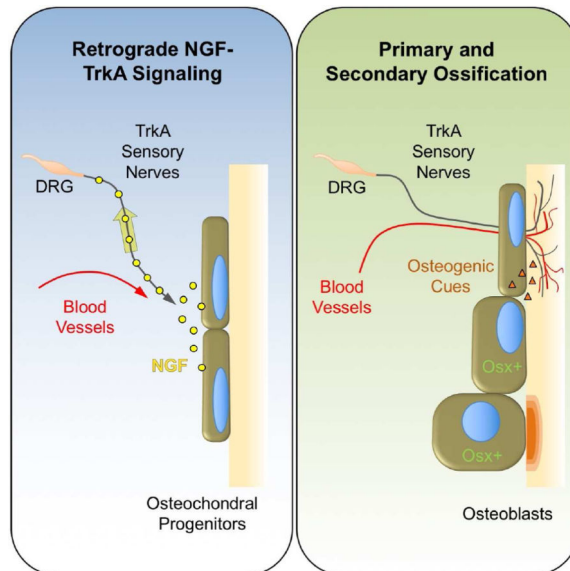
SUPPLEMENTAL INFORMATION

Supplemental information, including seven figures and two tables, can be found with this article online.

AUTHOR CONTRIBUTIONS

Conceptualization, R.E.T, T.M.B., L.M., F.Z., A.V., and T.L.C.; Investigation, R.E.T., Z.L, Q.Z., B.C.G., Z.L, D.L.J.T., and L.R.; Writing – Original Draft, R.E.T. and T.L.C.; Writing – Review & Editing, R.E.T. and T.L.C.; Supervision, T.L.C. The authors have no conflict of interest.

Graphical Abstract



Keywords

sensory nerves; endochondral bone; nerve growth factor; neurotrophic tyrosine kinase receptor type 1

INTRODUCTION

The formation of the vertebrate skeleton requires the action of both intrinsic and extrinsic inductive factors from multiple cell types, which function in a hierarchical and temporal fashion to control skeletal patterning and osteogenic progenitor differentiation (Olsen et al., 2000). During the development of endochondral bones of the limbs, osteochondral precursor cells in mesenchymal condensates differentiate into chondrocytes, forming an anlage that defines the site and dimension of the mature bone. Distinct groups of these mesenchymal cells form discrete layers at the periphery of the anlage, giving rise to the perichondrium. Fate mapping studies have shown compelling evidence that chondrocyte descendants inhabit the perichondrium and commit to the osteoblast lineage under the control of Osterix (Osx) and Runx2 (Kronenberg, 2003). Subsequent inductive cues (e.g. VEGF) produced by hypertrophic chondrocytes promote blood vessel invasion of the cartilaginous template, providing a conduit for cells and nutrients to arrive at the sites of primary ossification (Gerber et al., 1999).

Developing peripheral tissues dictate the amount and type of innervation they require by secreting specific neurotrophins, which promote neuronal survival by activating distinct tyrosine kinase receptors (Reichardt, 2006). The prototypic target tissue-derived neurotrophin is nerve growth factor (NGF), which activates its high affinity receptor neurotrophic tyrosine kinase receptor type 1 (TrkA) to initiate signaling that supports the survival of neurons (Huang and Reichardt, 2003). This function is facilitated by the

formation of NGF-TrkA endosomes, specialized signaling vesicles that undergo long-distance retrograde transport from the distal axon to the cell body via a microtubule-based transport mechanism (Harrington et al., 2011; Howe and Mobley, 2005; Howe et al., 2001). In addition, phosphorylation of TrkA at the axon tip or cell body can initiate a diverse array of signals that impact functions ranging from pain sensation to metabolic regulation (Kaplan and Stephens, 1994; Scita et al., 2000).

In contrast to the large body of literature on the role of peripheral nerves in the development of other tissues (Kumar and Brookes, 2012; Li et al., 2007), relatively few studies have investigated the function of peripheral nerves in the developing skeleton. Primary afferent sensory and sympathetic axons are known to cover the entire periosteal bone surface, are present in mineralized bone at the regions of highest metabolic activity, and reach deep into the marrow space (Bjurholm et al., 1988; Hill and Elde, 1991; Hukkanen et al., 1992; Mach et al., 2002; Wojtys et al., 1990). Importantly, the vast majority of nerves in mature bone are thinly myelinated or unmyelinated sensory neurons that express TrkA (Castaneda-Corral et al., 2011; Jimenez-Andrade et al., 2010). Early studies demonstrated that sciatic nerve resection in rats reduced longitudinal bone growth and impaired fracture healing (Garces and Santandreu, 1988; Madsen et al., 1998). In addition, mice treated with capsaicin to chemically destroy sensory nerves exhibited decreased bone volume along with reduced pain sensation (Heffner et al., 2014; Offley et al., 2005). These findings in rodents are consistent with reports from human studies that found patients with poor nerve function have delayed or abnormal skeletal repair (Nagano et al., 1989; Santavirta et al., 1992). While such studies provide circumstantial support for sensory nerve function in bone, the extent to which sensory nerve-derived signals directly influence bone development is unknown.

In this study, we used mouse models to visualize and disrupt the functional signaling of the specific sensory nerves that innervate the skeleton. Our results show that NGF expression in the developing endochondral bone coincides with vascularization and osteochondral progenitor cell expansion. Inhibition of TrkA signaling or deletion of NGF in perichondrial osteochondral precursor cells over this time frame disrupts ossification of the primary and secondary ossification centers and impairs postnatal bone mass and length.

RESULTS

Innervation of the developing mouse femur by TrkA sensory nerves coincides with primary ossification

To determine the timing and location of sensory nerve invasion of the developing mouse skeleton, we used two well-characterized reporter mice: TrkA-LacZ mice, in which one TrkA allele has been replaced with a LacZ construct (Moqrich et al., 2004), and the pan-neuronal Thy1-YFP mouse that expresses yellow fluorescent protein (YFP) under the control of neuron-specific elements from the *Thy1* gene (Feng et al., 2000). We concentrated on the hindlimb, in which endochondral ossification of the cartilaginous rudiments begins around embryonic day 15 in the mouse. X-gal staining of optically cleared embryos harvested from timed pregnant TrkA-LacZ mice revealed LacZ positive axons innervating the hindlimb via the lumbar plexus by nerves from L1 to L6 (Fig. 1 A–D). Moreover, LacZ positive neuronal projections were observed extending into the limb and terminating near the

perichondrial region of the femur as early as embryonic day 14.5 (Fig. 1 E, arrow). At later times in embryogenesis and postnatal life, the TrkA sensory nerve bundles were progressively larger and more clearly defined with a similar overall pattern (Fig. 1 F–H). In a parallel study, optically cleared embryos from Thy1-YFP mice were imaged using confocal microscopy to reveal greater detail at the site of sensory nerve contact (Fig. 1 I–L). The results from the Thy1-YFP mice showed an identical timing and innervation pattern as that seen in the TrkA-LacZ mouse, in agreement with previous reports that the sensory nerves in the mouse skeleton mainly express TrkA (Castaneda-Corral et al., 2011). Confocal imaging of whole-mounted and cleared hind limbs with muscle removed revealed thin YFP positive axonal projections terminating at the perichondrial surface adjacent to sites of incipient ossification at E14.5 (Fig. 1 M). By E16.5, YFP positive axons densely covered the perichondrial surface, and became more abundant by E18.5 (Fig. 1 N, O). By postnatal day 0, thin nerve projections had covered the entire mineralizing bone collar, but ended at the growth plate, with no axons observed extending into the cartilaginous ends (Fig. 1 P).

NGF expression in perichondrial cells adjacent to the femoral primary ossification center

As discussed above, NGF has been identified as the neurotrophin for TrkA sensory nerves and acts through retrograde signaling to promote neuronal survival and provide axon guidance. Therefore, we determined the pattern of NGF expression in developing femurs over the time period of TrkA innervation using a previously validated NGF-eGFP reporter mouse (Kawaja et al., 2011). In the developing femur, NGF expression was first observed at E14.5 in small discrete groups of perichondrial cells immediately adjacent to the site of incipient mineralization in the primary ossification center (Fig. 2 A). Immunohistochemistry was performed against PECAM1 (CD31) to mark invading vasculature and against Osterix/Sp7 (Osx) to mark prehypertrophic chondrocytes and osteoblast lineage cells. Expression of NGF by perichondrial cells was observed as early as embryonic day 14.5 (Fig. 2 B), preceding vascular invasion of the primary ossification center (Fig. 2 C). At this time point, Osx-expressing chondrocytes were observed in primary ossification center as well as in the perichondrium, where they were adjacent to NGF-expressing cells (Fig. 2 D, arrow). At later embryonic time points (E16.5 and E18.5), NGF was no longer expressed exclusively in the perichondrial region and was abundant on newly forming trabecular bone surfaces within the primary ossification center (Fig. S1). A similar pattern of NGF expression in the developing mouse femur over this developmental time frame was observed using immunohistochemistry with antibodies against NGF (Fig. S2). Immediately following birth, NGF expression remained robust on bone surfaces within the developing bone (Fig. 2 E). At the femoral metaphysis, NGF-expressing cells (Fig. 2 F) did not appear to be associated with vasculature, as visualized by CD31 expression (Fig. 2 G). Although some NGF-expressing cells in the femoral metaphysis were closely associated with Osx-expressing cells (Fig. 2 H, arrows), most cells expressing NGF at this time point were not. By postnatal day 7, NGF expression in the developing limb had generally declined throughout the bone with the exception of limited expression at the growth plate (Fig. S3), consistent with the downregulation of TrkA in the DRG during this time frame (Molliver and Snider, 1997). Brain sections were used as a positive control for NGF expression in NGF-eGFP mice (*not shown*). Consistent with the expression of NGF *in vivo*, analysis of NGF mRNA in both primary osteoblasts and mesenchymal stromal cells (MSCs) *in vitro* showed high levels of

expression in freshly plated cells, which fell to a baseline level as cells differentiated (Fig. S5 A). Collectively, these results are compatible with our hypothesis that NGF expressed by perichondrial cells acts as the neurotrophic agent for the innervation of the skeleton, resulting in adult bones that are predominantly occupied by TrkA sensory nerves.

Inhibition of TrkA signaling in sensory nerves attenuates innervation, vascularization, and primary ossification

Mice with the unrestricted loss of TrkA die shortly after birth with severe neuropathies (Crowley et al., 1994; Smeyne et al., 1994), limiting their utility for studying the role of NGF-TrkA signaling. To circumvent these problems, we used a mouse in which TrkA signaling can be acutely disrupted over defined windows of time. TrkA^{F592A} mice are homozygous for TrkA knockin alleles that encode a phenylalanine-to-alanine substitution in the protein kinase subdomain V, rendering its catalytic activity sensitive to specific inhibition by the membrane-permeable, small molecule 1NMPP1 (Chen et al., 2005). To validate this model, we determined the effect of 1NMPP1 on dissociated DRG neurons harvested from E13.5 TrkA^{F592A} mice and cultured in microfluidic chambers (Fig. 3 A). Treatment of neuronal preparations with 1NMPP1 attenuated the NGF-dependent axonal outgrowth of these neurons in a dose-dependent fashion (Fig. 3 B–E). In separate experiments, mouse MSCs expressing a GFP reporter were transfected with an NGF expression plasmid or control plasmid and plated in microfluidic chambers opposite of DRG neurons cultured in media containing suboptimal NGF. In this setting, axonal infiltration was significantly increased in cultures of NGF-transfected MSCs (Fig. 3 F–H). The ability of 1NMPP1 to inhibit TrkA in vivo was confirmed by the marked reduction in TrkA phosphorylation 24 hours after a single IP injection of 1NMPP1 (17 ug/g BW) in intact DRGs by immunohistochemistry (Fig. 3 I, J) and by immunoblotting of DRG extracts (Fig. 3 K, L). To determine the effect of inhibiting TrkA signaling during embryogenesis, pregnant heterozygous (TrkA^{F592A/wt}) mice that carried the Thy1-YFP transgene were provided drinking water containing 1NMPP1 (40 uM), starting at the time of mating and continuing until birth. TrkA^{F592A};Thy1-YFP offspring exhibited decreased DRG size with altered morphology (Fig. 3 M–O) as well as diminished skin innervation at birth as compared to TrkA^{wt};Thy1-YFP littermate controls (Fig. 3 P–R).

Using this protocol, we next determined the effect of TrkA inhibition on femur development in the immediate postnatal period. TrkA^{F592A};Thy1-YFP mice had significantly reduced density of Thy1-YFP+ nerves in the distal metaphysis of the femur (Fig. 4 A–D). This result was confirmed by immunohistochemistry against the pan-neuronal marker PGP9.5 (Fig. S4 A – C) as well as against TrkA (Fig. S4 D – F). Furthermore, TrkA^{F592A};Thy1-YFP mice had significantly reduced vascular density at the distal metaphysis of the femur, as indicated by CD31 staining (Fig. 4 E–H). Analysis of H&E stained sections showed no gross defects in organization or size of the growth plate in TrkA^{F592A};Thy1-YFP mice (Fig. 4 I–L). However, skeletal preparations using alizarin red and alcian blue revealed shorter and thinner femurs in TrkA^{F592A};Thy1-YFP mice as compared to TrkA^{wt};Thy1-YFP littermates (Fig. 4 M, N). This result was quantitatively confirmed by microCT analysis, in which TrkA^{F592A};Thy1-YFP mice displayed significantly diminished femoral length (–11%, –12%), reduced overall bone volume (–20%, –22%), and decreased polar moment of inertia

(−24%, −30%) at postnatal days 0 and 7, respectively (Fig. 4 O–T). We are unable to attribute the alterations in bone morphology observed in $\text{TrkA}^{\text{F592A}};\text{Thy1-YFP}$ mice to a direct effect of 1NMPP1 on osteoblasts, since primary osteoblasts and MSCs both have low or undetectable TrkA mRNA expression (Fig. S5 B) and increasing concentration of 1NMPP1 in differentiation media containing NGF did not affect alkaline phosphatase or alizarin red staining of primary osteoblast cultures after either 14 or 21 days of differentiation (Fig. S5 C, D).

The close temporal and spatial relationship between TrkA innervation and perichondrial osteochondral progenitors in the developing femur (Fig. 1, 2) led us to hypothesize that delayed innervation may delay vascular invasion and/or reduce the osteoprogenitor pool during primary ossification. Therefore, we examined femurs harvested from mice at embryonic day 15.5, a time at which hypertrophic chondrocytes have begun to undergo their apoptotic program that facilitates vascular invasion (Kronenberg, 2003). Femurs from $\text{TrkA}^{\text{F592A}};\text{Thy1-YFP}$ mice had significantly diminished Thy1-YFP^+ nerves located in the perichondrial region (Fig. 5 A–C). Moreover, vascular invasion of the primary ossification center was impaired in the $\text{TrkA}^{\text{F592A}};\text{Thy1-YFP}$ mice as visualized by CD31 staining (Fig. 5 D–F). Finally, $\text{TrkA}^{\text{F592A}};\text{Thy1-YFP}$ mice had a significantly diminished pool of cells expressing the transcription factor Osterix (Osx), which is known to mark perichondrial cells that invade the cartilaginous template to become both osteoblasts and stromal cells (Maes et al., 2010) (Fig. 5 G–I).

Disruption of NGF in perichondrial osteochondral precursors attenuates femoral innervation, vascularization, and ossification

The upregulation of NGF by perichondrial cells coincident with the first TrkA axons reaching the developing long bone suggested that NGF expressed by these cells functioned as a skeletal neurotrophic factor. Therefore, we hypothesized that genetic deletion of NGF in these cells should yield a bone phenotype analogous to that seen in $\text{TrkA}^{\text{F592A}};\text{Thy1-YFP}$ mice. To explore this idea, mice with floxed NGF alleles ($\text{NGF}^{\text{fl/fl}}$) (Muller et al., 2012) were mated to mice carrying $\text{Col2-CreER}^{\text{T}}$, a construct which has been used extensively to map the fate of early perichondrial precursors (Ono et al., 2014). Tamoxifen (1 mg) and progesterone (1 mg) were administered to timed pregnant mice at embryonic day 11.5, a time point at which recombination occurs throughout the developing limb, including the proliferating cartilage and perichondrium (Nakamura et al., 2006). Femurs from $\text{NGF}^{\text{fl/fl}}$ and $\text{NGF}^{\text{fl/fl}};\text{Col2-CreER}^{\text{T}}$ littermates were harvested for analysis. First, immunohistochemistry against NGF was used to confirm the complete loss of NGF throughout the developing bone in $\text{NGF}^{\text{fl/fl}};\text{Col2-CreER}^{\text{T}}$ mice (Fig. 6 A–D). Next, staining using antibodies against PGP9.5 (Fig. 6 E–H) and TrkA (Fig. S6 A – C) revealed decreased metaphyseal innervation in femurs from $\text{NGF}^{\text{fl/fl}};\text{Col2-CreER}^{\text{T}}$ mice. In addition, femurs from $\text{NGF}^{\text{fl/fl}};\text{Col2-CreER}^{\text{T}}$ mice had diminished vascularization of the distal metaphysis, as illustrated by immunohistochemistry against CD31 (Fig. 6 I–L). Similar to the results from $\text{TrkA}^{\text{F592A}};\text{Thy1-YFP}$ mice, H&E stained sections in $\text{NGF}^{\text{fl/fl}};\text{Col2-CreER}^{\text{T}}$ mice did not reveal any gross defects in organization or size of the growth plate (Fig. 6 M–P). Finally, femurs from $\text{NGF}^{\text{fl/fl}};\text{Col2-CreER}^{\text{T}}$ mice at postnatal day 0 were shorter (−8%) with significantly diminished bone volume (−17%) as quantified by microCT (Fig. 6 Q–T). These

results are entirely compatible with the conclusion that NGF expression by perichondrial osteochondral precursors drives TrkA signaling in sensory nerves to mediate primary ossification.

TrkA signaling is required for formation of secondary ossification centers in the developing femur

During the course of these studies, we noted that mineralization of the secondary ossification center (SOC) in femurs from TrkA^{F592A};Thy1-YFP mice was delayed compared to TrkA^{wt};Thy1-YFP littermates (Fig. 4 M, N). Formation of the SOC in the murine femur occurs around postnatal day 5, involves the hypertrophic differentiation of epiphyseal chondrocytes, and requires the formation of vascular canals (also known as cartilage canals) (Dao et al., 2012; Xing et al., 2014). These structures form at the perichondrial surface of the epiphysis at birth and ultimately penetrate to center of the epiphysis to create a conduit for blood vessels and mesenchymal progenitor cells (Cole and Wezeman, 1985; Kugler et al., 1979; Lutfi, 1970). Close inspection of hind limbs from TrkA-LacZ⁺ mice harvested at postnatal day 0 indicated TrkA sensory axons were present at the epiphyseal surface of the femur and tibia at the time of vascular canal formation (Fig. 7 A, arrowheads). Intact hind limbs from NGF-eGFP mice harvested at postnatal day 0 revealed cells expressing NGF at the leading front of nascent vascular canals (Fig. 7 B, C) as well as at positions of putative canal formation (Fig. 7 D, E). Furthermore, cells expressing NGF were abundant throughout the enlarged vascular canals tunneling towards the nascent secondary ossification center by postnatal day 7 (Fig. 7 F, G). In addition, Thy1-YFP⁺ nerves from the epiphyseal surface were observed entering and inhabiting epiphyseal vascular canals (Fig. 7 H, I), but were distinctly absent from areas of the epiphysis that had not been invaded (Fig. 7 I, asterisks). To investigate the role that NGF-TrkA signaling may play in the formation of epiphyseal vascular canals and subsequent secondary ossification, offspring of pregnant heterozygous (TrkA^{F592A/wt}) mice that had been provided drinking water containing INMPP1 (40 uM) from mating until sacrifice were analyzed. In TrkA^{F592A};Thy1-YFP offspring, vascular canals at postnatal day 7 were present, vascularized, and innervated, but were greatly reduced in size as compared to TrkA^{wt};Thy1-YFP littermates (Fig. 7 J, K). Furthermore, TrkA^{F592A};Thy1-YFP mice had significantly reduced secondary ossification bone volume, as illustrated by skeletal preparations (Fig. 7 L–M) and quantified by microCT (Fig. 7 N–Q) at day 7 (–75%) and day 14 (–38%). These results illustrate that NGF-TrkA signaling plays an essential role in secondary ossification by a mechanism similar to that observed during primary ossification.

DISCUSSION

In this study, we used several genetic mouse models to identify the sensory nerves that innervate the developing mouse femur and determine their spatiotemporal relationship to early osteogenic events. We show that TrkA signaling by these sensory nerves is essential for early innervation and is required for the normal formation of both primary and secondary ossification centers. Moreover, we provide firm evidence that NGF produced by osteochondral progenitors functions as a skeletal neurotrophin by activating TrkA, which directs sensory nerve axons to sites of incipient ossification. These conclusions are supported

by several observations. First, TrkA axons emanating from the DRG innervated sites of incipient primary ossification, coincident in time and space with the appearance of NGF expression in the adjacent perichondrial cells. These events were recapitulated at the secondary ossification center, an independent site of postnatal bone formation. Importantly, inhibition of TrkA signaling or genetic deletion of NGF from perichondrial osteochondral progenitor cells over this developmental time frame produced virtually identical femoral phenotypes, characterized by reduced skeletal innervation, vascularization, and bone mass at birth. We attribute these phenotypes to the loss of TrkA signaling in sensory nerves, despite the fact that the chemical-genetic approach used here would inhibit TrkA signaling in all cell types that express the receptor. In this regard, the ability to precisely control the timing of TrkA inhibition over a narrow developmental time frame is critical to our conclusion that sensory nerves are the primary target. Thus, the majority of non-neuronal cells present at this early stage of bone development are mesenchymal osteochondral progenitors, which do not express TrkA (Fig. S5). Furthermore, the few TrkA sympathetic nerve fibers that may be present at this developmental time point would not yet be functioning to control vascular tone (Brunet et al., 2014).

The requirement of NGF-TrkA signaling in sensory nerves for the proper development of endochondral bone is entirely consistent with the neurotrophic hypothesis that states that the expression of neurotrophins in target tissues determines the type and density of invading nerves (Davies et al., 1987; Levi-Montalcini and Angeletti, 1968). In addition, our work demonstrates that these TrkA sensory nerves assist in the vascular invasion of both primary and secondary ossification sites. In this regard, our results are compatible with previous studies in developing skin, which have shown that signals from nascent TrkA sensory nerves provide essential cues necessary for patterning arterial blood vessel branching during cutaneous vascularization (Mukouyama et al., 2002). This process may be facilitated directly through NGF-TrkA signaling, since NGF itself is capable of inducing VEGF expression in peripheral sensory nerves by activating TrkA (Calza et al., 2001). In addition to vascularization, our results suggest that sensory nerves may provide osteogenic cues that promote osteoblast lineage progression by increasing the number of cells in the primary ossification center that express Osterix (Osx) (Nakashima et al., 2002). Along these lines, sensory nerves in the adult hair follicle were shown to release Sonic Hedgehog (Shh) to maintain the stem cell niche necessary for skin homeostasis as well as acute wound healing (Brownell et al., 2011). More recently, a similar process has been observed in the development of the rodent incisor, during which the alveolar sensory nerve within the neurovascular bundle releases Shh that acts to support the differentiation of periarterial stem cells (Zhao et al., 2014). Whether or to what extent TrkA sensory nerves in bone release Shh, or any other signaling molecule, is unknown. Because of the direct association between invading vasculature and osteoprogenitors that may be independent of innervation (Maes et al., 2010), it is possible that sensory nerves only play a permissive role to enable vascularization during ossification, rather than actively signaling to skeletal cells. Thus, the precise mechanism that links NGF-TrkA signaling to downstream events regulating endochondral bone formation remains to be determined.

In this study, we showed that diminished NGF-TrkA signaling decreases the total volume of bone acquired during embryogenesis. During this relatively narrow window of time, the

skeleton is rapidly being formed and mineralized through the action of osteoblasts. Although osteoclasts are present at ossification sites, their contribution to the overall bone volume is minimal. As a result, our study design focused on osteoblast-related events, revealing that NGF-TrkA signaling is required for normal accumulation of Osterix-expressing osteoprogenitor cells (Fig. 5C). To address the possibility that osteoclasts were similarly affected, we quantified TRAP staining in TrkA^{F592A};Thy1-YFP, NGF^{fl/fl};Col2-CreER^T, and control newborn mice (Fig. S7). Although we observed no differences in osteoclast number, these data are entirely compatible with our conclusion that loss of NGF-TrkA signaling reduces bone mass primarily by attenuating bone formation.

It is important in the context of this paper to discuss several studies that examined the skeletal action of semaphorin 3A (Sema3A), a well-characterized inhibitor of neuronal outgrowth that is expressed in bone and cartilage. Mice with the unrestricted loss of Sema3A were observed to have gross defects in the patterning and growth of the nerves, heart, and skeleton (Behar et al., 1996), leading to subsequent work showing that Sema3A is an osteoblast-derived factor that can suppress osteoclastogenesis (Hayashi et al., 2012). However, although the specific deletion of Sema3A in the osteoblast lineage did not affect either sensory innervation or bone volume, mice lacking Sema3A selectively in neurons have decreased sensory innervation of bone and diminished postnatal bone mass (Fukuda et al., 2013). In light of our results, we hypothesize that the loss of Sema3A, either globally or selectively in neurons, disrupts TrkA sensory neuron organization in a non-specific manner, potentially affecting skeletal vascularization and/or osteochondral progenitors and leading to defects in postnatal bone acquisition.

Finally, there is considerable circumstantial evidence that TrkA sensory nerves function in the development and maintenance of human bone. For example, mutations in the *TRKA* gene cause congenital insensitivity to pain with anhidrosis (CIPA) (Indo et al., 1996), an autosomal recessive syndrome associated with skeletal disorders such as short stature, tooth loss, and delayed fracture healing (Bonkowsky et al., 2003; Toscano et al., 2000). Similarly, patients with familial dysautonomia (FD) have progressive sensory neuron loss and low bone mass (Jackson et al., 2014), as do children with perinatal brachial plexus palsy (PBPP), a flaccid paralysis of the arm caused by nerve damage at birth (Ibrahim et al., 2011). Finally, individuals with spinal cord injury commonly develop osteopenia (Edwards et al., 2014; Garland et al., 1992). These observations in humans are entirely compatible with our findings in mice and underscore the need for further investigation of the function of the peripheral nervous system in the human skeleton.

EXPERIMENTAL PROCEDURES

Mice

All procedures involving mice were approved by the Institutional Animal Care and Use Committee of The Johns Hopkins University (protocol #M015M118). TrkA^{F592A} mice are homozygous for a phenylalanine-to-alanine point mutation in exon 12 of the mouse *Ntrk1* gene (F592A), rendering the endogenous TrkA kinase sensitive to inhibition by the membrane-permeable small molecule INMPP1 (Chen et al., 2005). TrkA^{F592A} mice are commercially available (Jackson Laboratory, Stock #022362). TrkA-LacZ mice, which have

a LacZ sequence inserted immediately downstream of the ATG in exon 1 of the mouse *Ntrk1* gene (Moqrich et al., 2004), are commercially available (Jackson Laboratory, Stock #004837). Thy1-YFP mice, which harbor a transgene derived from the mouse *Thy1* gene that directs expression of YFP in motor and sensory neurons (Feng et al., 2000), are commercially available (Jackson Laboratory, Stock #003709). NGF-eGFP mice, which express eGFP under the control of the mouse *NGF* promoter, were generously donated by the Kawaja lab (Kawaja et al., 2011). Mice with floxed NGF alleles were generated in the Minichiello lab (Muller et al., 2012). Col2-CreER^T mice, which can be induced by tamoxifen to express Cre recombinase in cells that express Type II collagen (Nakamura et al., 2006), are available commercially (Jackson Laboratory, Stock #006774). Littermate analysis was performed while blinded to genotype.

Synthesis and Administration of 1NMPP1

1NMPP1 (Lot #51-180-51) was synthesized by Aurora Analytics LLC using standard techniques (Hanefeld et al., 1996). Purity (99.2%) was confirmed by HPLC-UV254, and characterization by ¹H NMR (400 MHz, DMSO-d₆) was consistent with structure. Stock solution was prepared at 200 mM by dissolving 1NMPP1 powder in DMSO. IP injections were performed using a 5 mM solution at a dosage of 17 ug/g BW. Drinking water was prepared at 40 uM in ddH₂O with 1% PBS-Tween 20.

X-Gal Staining

Whole embryos were harvested on ice, then fixed for 8 hours at 4 °C in 0.2% glutaraldehyde containing 5mM EGTA, 10 mM MgCl₂, and 100 mM NaH₂PO₄ (pH 7.3). Following this, each specimen was stained overnight at 4 °C in X-gal solution containing 20 mM Tris-HCl (pH 7.5) with 1 mg/mL X-Gal, 5 mM Potassium Ferricyanide, and 5 mM Potassium Ferrocyanide. After post-fixation in 4% PFA at 4 °C overnight, the embryos were cleared using increasing concentrations of glycerol (20%, 50%, 80%), brought to final volume with 1% KOH. Finally, each embryo was placed in 100% glycerol for imaging using a digital camera and macro lens (Fujifilm XT-1, 60 mm f2.4).

Skeletal Preparation

Whole embryos were harvested on ice to remove skin and eviscerate organs. The samples were incubated overnight in each 100% ethanol and 100% acetone. Next, samples were placed in a solution containing 0.03% Alcian Blue (Sigma A5268) in 80% ethanol and 20% glacial acetic acid (Sigma A6283) for 16–24 hours. After sufficient cartilaginous staining, samples were washed in 70% ethanol for two hours and 95% ethanol overnight. Following this, samples were placed in a 1% potassium hydroxide (KOH) solution for 1 hour at room temperature. Next, samples were placed in a solution containing 0.005% Alizarin Red (Sigma A5533) in 1% KOH for 3–4 hours. Finally, samples were incubated in a solution containing 50% glycerol in 1% KOH until clear, then imaged and stored in 100% glycerol.

Clearing and Confocal Imaging

Samples were harvested under a dissecting microscope to remove soft tissue, then placed in 4% PFA at 4 °C for 16–24 hours. After 3 washes in PBS and decalcification in 14% EDTA

(1:20 volume) for up to 14 days at 4 °C, samples were optically cleared using a modified SeeDB method (Ke and Imai, 2014). Briefly, samples were immersed in increasing concentrations of D-(–)-Fructose (F3510, Sigma), with 0.5% α -thioglycerol (M1753, Sigma), up to a maximum concentration of 80.2% (wt/wt) fructose with gentle shaking at room temperature. After obtaining sufficient clarity, intact samples were mounted on coverslips and imaged using confocal microscopy (Zeiss 780 LSM).

Histology

Intact hindlimbs were harvested and placed in 4% PFA at 4 °C for 16–24 hours. After 3 washes in PBS, samples were decalcified in 14% EDTA (1:20 volume) for up to 14 days at 4 °C. Next, samples were sunk in 30% sucrose overnight at 4 °C before embedding in O.C.T. media (Tissue-Tek). Sections were cut and mounted on adhesive slides (TruBond 380). For immunohistochemistry, sections were allowed to dry overnight, thoroughly washed, blocked using PBS with 1.5% normal serum, and incubated in primary antibody (Table S1) overnight at 4 °C in a humidified chamber. The following day, slides were washed, incubated in fluorescent secondary antibody for 1 hour at 4 °C, then mounted using media containing DAPI (Vectashield H-1200). Digital images of these sections were captured using bright field microscopy (Olympus IX-71) with a 10 \times or 20 \times objective. Imaging stitching and quantification was performed using FIJI (Schindelin et al., 2012).

MicroCT Analysis

Bones were dissected free of soft tissue and evaluated using a SkyScan1172 (Bruker) high-resolution microcomputed tomography imaging system. Each bone was scanned separately at 65 kV and 170 μ A with a 0.5-mm aluminum filter to obtain a 10.9 μ m voxel size. Scan slices were acquired in the transverse plane by placing the bone parallel to the z-axis of the scanner. NRecon (Bruker) was used to reconstruct images using a beam hardening correction of 40%, and quantitative analysis was performed using CTAn (Bruker) in accordance with the recommendations of the American Society for Bone and Mineral Research (Bouxsein et al., 2010).

Osteoblast culture

Osteoblasts were isolated from calvaria of newborn mice as previously described (Fulzele et al., 2010). Osteoblasts were incubated in a 37 °C humidified incubator at 5% CO₂. Osteoblasts were cultured to confluency and differentiated in medium supplemented with 10 mM β -glycerol phosphate, 50 μ g/mL ascorbic acid, and varying concentrations of 1NMPP1 or equal volume DMSO. Osteoblast cultures were fixed using 100% ethanol. Alkaline phosphatase activity and mineralization was determined after 14 or 21 days of differentiation by staining with Fast Red TR/Naphthol AS-MX phosphate (Sigma) or 40 mM Alizarin Red (Sigma), respectively.

Microfluidic Platform Assays

Microfluidic platforms, consisting of a poly-dimethylsiloxane (PDMS) device bonded to a glass coverslip, were generated as previously described (Hosmane et al., 2012). Briefly, two layers of photoresist structures were generated on a flat silicon wafer – one for the 100 μ m

cell chambers (SU-8 3050) and one for the 3 μm microgrooves (SU-8 2002). After pouring PDMS over the master mold and incubating for 1 hour at 37 °C, access ports were created using dermal biopsy punch tools (Huot Instrument). Finally, each device was sterilized with 70% ethanol before plasma bonding to a sterile glass coverslip and incubating overnight with a 200 $\mu\text{g}/\text{mL}$ solution of poly-D-lysine (Sigma). For the DRG infiltration assay, DRGs were harvested from mice at embryonic day 13.5 into ice-cold culture medium (DMEM/F-12 supplemented with 5% FBS, 1 \times penicillin/streptomycin, and 50 ng/mL NGF), as previously described (Lentz et al., 1999). Next, DRGs were digested with 1 mg/mL collagenase A (Roche) at 37 °C for 15 minutes, and then with 0.05% trypsin-EDTA at 37 °C for 7 minutes. Following this, DRGs were washed three times with culture medium and dissociated by trituration with 1 mL pipette tip. The dissociated neurons were plated into the microfluidic devices at a density of 10^4 neurons/ cm^2 . Non-neuronal cells were eliminated using 20 μM 5-fluoro-2-deoxyuridine and 20 μM uridine (FDU/R). Neurons were cultured for 72 hours and stained with CellTracker CMTX Dye (Life Technologies). For co-culture of DRG neurons with MSCs, MSCs were transfected with mouse NGF expression vector (MG225454, Origene) using Lipofectamine 3000 (Thermo Fisher Scientific) at 1.6 $\mu\text{g}/10^6$ MSCs. Separately, DRG neurons were cultured in the middle microfluidic chamber as described above. Four hours after transfection (20 hours after starting DRG culture), the MSCs were trypsinized and resuspended in complete medium containing suboptimal NGF (2.5 ng/mL). Finally, 10^4 MSCs were plated into the outer compartments of the microfluidic device.

Gene Expression by qRT-PCR

Total RNA was collected from primary osteoblasts harvested from neonates (as above) or MSCs (Texas A&M Health Science Center College of Medicine Institute for Regenerative Medicine at Scott & White) after 0, 7, and 14 days of differentiation using TRIzol (Life Technologies) according to the manufacturer's protocol. RNA (1 μg) was then reversely transcribed using an iScript cDNA Synthesis Kit (Bio-Rad). cDNA (2 μL) was then amplified under standard PCR conditions using iQ SYBR Green Supermix (Bio-Rad). All cDNA samples were run in triplicate, averaged, and normalized to endogenous β -actin expression levels. Primer sequences (Table S2) were designed using Primer-BLAST (NCBI).

Statistics

All results are presented as mean \pm standard error. Statistical analyses were performed in Prism (GraphPad) using unpaired, two-tailed Student's t-tests. A p-value of less than 0.05 was considered significant.

Supplementary Material

Refer to Web version on PubMed Central for supplementary material.

Acknowledgments

This work was supported by grants from the National Institutes of Health: AR068934 (TC) and NS085176 (FZ). TC is the recipient of a Senior Career Scientist Award from the Department of Veterans Affairs and FZ is supported by The Craig H. Nielsen Foundation. The authors thank Drs. David Ginty, Michael Kawaja, and Aziz Moqrigh for

supplying mice used in this study, Drs. Alex Kolodkin and Richard Haganir for helpful discussions, Julie Frey for help with injections, and Michele Doucet for assistance with histology.

REFERENCES

- Behar O, Golden JA, Mashimo H, Schoen FJ, Fishman MC. Semaphorin III is needed for normal patterning and growth of nerves, bones and heart. *Nature*. 1996; 383:525–528. [PubMed: 8849723]
- Bjurholm A, Kreicbergs A, Brodin E, Schultzberg M. Substance P- and CGRP-immunoreactive nerves in bone. *Peptides*. 1988; 9:165–171. [PubMed: 2452430]
- Bonkowsky JL, Johnson J, Carey JC, Smith AG, Swoboda KJ. An infant with primary tooth loss and palmar hyperkeratosis: a novel mutation in the NTRK1 gene causing congenital insensitivity to pain with anhidrosis. *Pediatrics*. 2003; 112:e237–e241. [PubMed: 12949319]
- Bouxsein ML, Boyd SK, Christiansen BA, Guldberg RE, Jepsen KJ, Muller R. Guidelines for assessment of bone microstructure in rodents using micro-computed tomography. *J Bone Miner Res*. 2010; 25:1468–1486. [PubMed: 20533309]
- Brownell I, Guevara E, Bai CB, Loomis CA, Joyner AL. Nerve-derived sonic hedgehog defines a niche for hair follicle stem cells capable of becoming epidermal stem cells. *Cell stem cell*. 2011; 8:552–565. [PubMed: 21549329]
- Brunet I, Gordon E, Han J, Cristofaro B, Broqueres-You D, Liu C, Bouvree K, Zhang J, del Toro R, Mathivet T, et al. Netrin-1 controls sympathetic arterial innervation. *J Clin Invest*. 2014; 124:3230–3240. [PubMed: 24937433]
- Calza L, Giardino L, Giuliani A, Aloe L, Levi-Montalcini R. Nerve growth factor control of neuronal expression of angiogenetic and vasoactive factors. *Proc Natl Acad Sci U S A*. 2001; 98:4160–4165. [PubMed: 11259645]
- Castaneda-Corral G, Jimenez-Andrade JM, Bloom AP, Taylor RN, Mantyh WG, Kaczmarek MJ, Ghilardi JR, Mantyh PW. The majority of myelinated and unmyelinated sensory nerve fibers that innervate bone express the tropomyosin receptor kinase A. *Neuroscience*. 2011; 178:196–207. [PubMed: 21277945]
- Chen X, Ye H, Kuruvilla R, Ramanan N, Scangos KW, Zhang C, Johnson NM, England PM, Shokat KM, Ginty DD. A chemical-genetic approach to studying neurotrophin signaling. *Neuron*. 2005; 46:13–21. [PubMed: 15820690]
- Cole AA, Wezeman FH. Perivascular cells in cartilage canals of the developing mouse epiphysis. *Am J Anat*. 1985; 174:119–129. [PubMed: 4061338]
- Crowley C, Spencer SD, Nishimura MC, Chen KS, Pitts-Meek S, Armanini MP, Ling LH, McMahon SB, Shelton DL, Levinson AD, et al. Mice lacking nerve growth factor display perinatal loss of sensory and sympathetic neurons yet develop basal forebrain cholinergic neurons. *Cell*. 1994; 76:1001–1011. [PubMed: 8137419]
- Dao DY, Jonason JH, Zhang Y, Hsu W, Chen D, Hilton MJ, O'Keefe RJ. Cartilage-specific beta-catenin signaling regulates chondrocyte maturation, generation of ossification centers, and perichondrial bone formation during skeletal development. *J Bone Miner Res*. 2012; 27:1680–1694. [PubMed: 22508079]
- Davies AM, Bandtlow C, Heumann R, Korsching S, Rohrer H, Thoenen H. Timing and site of nerve growth factor synthesis in developing skin in relation to innervation and expression of the receptor. *Nature*. 1987; 326:353–358. [PubMed: 3031505]
- Edwards WB, Schnitzer TJ, Troy KL. Bone mineral and stiffness loss at the distal femur and proximal tibia in acute spinal cord injury. *Osteoporos Int*. 2014; 25:1005–1015. [PubMed: 24190426]
- Feng G, Mellor RH, Bernstein M, Keller-Peck C, Nguyen QT, Wallace M, Nerbonne JM, Lichtman JW, Sanes JR. Imaging neuronal subsets in transgenic mice expressing multiple spectral variants of GFP. *Neuron*. 2000; 28:41–51. [PubMed: 11086982]
- Fukuda T, Takeda S, Xu R, Ochi H, Sunamura S, Sato T, Shibata S, Yoshida Y, Gu Z, Kimura A, et al. Sema3A regulates bone-mass accrual through sensory innervations. *Nature*. 2013; 497:490–493. [PubMed: 23644455]

- Fulzele K, Riddle RC, DiGirolamo DJ, Cao X, Wan C, Chen D, Faugere MC, Aja S, Hussain MA, Bruning JC, et al. Insulin receptor signaling in osteoblasts regulates postnatal bone acquisition and body composition. *Cell*. 2010; 142:309–319. [PubMed: 20655471]
- Garces GL, Santandreu ME. Longitudinal bone growth after sciatic denervation in rats. *The Journal of bone and joint surgery British volume*. 1988; 70:315–318. [PubMed: 3346314]
- Garland DE, Stewart CA, Adkins RH, Hu SS, Rosen C, Liotta FJ, Weinstein DA. Osteoporosis after spinal cord injury. *J Orthop Res*. 1992; 10:371–378. [PubMed: 1569500]
- Gerber HP, Vu TH, Ryan AM, Kowalski J, Werb Z, Ferrara N. VEGF couples hypertrophic cartilage remodeling, ossification and angiogenesis during endochondral bone formation. *Nat Med*. 1999; 5:623–628. [PubMed: 10371499]
- Hanefeld U, Rees CW, White AJP, Williams DJ. One-pot synthesis of tetrasubstituted pyrazoles - Proof of regiochemistry. *J Chem Soc Perk T*. 1996; 1:1545–1552.
- Harrington AW, St Hillaire C, Zweifel LS, Glebova NO, Philippidou P, Haleboua S, Ginty DD. Recruitment of actin modifiers to TrkA endosomes governs retrograde NGF signaling and survival. *Cell*. 2011; 146:421–434. [PubMed: 21816277]
- Hayashi M, Nakashima T, Taniguchi M, Kodama T, Kumanogoh A, Takayanagi H. Osteoprotection by semaphorin 3A. *Nature*. 2012; 485:69–74. [PubMed: 22522930]
- Heffner MA, Anderson MJ, Yeh GC, Genetos DC, Christiansen BA. Altered bone development in a mouse model of peripheral sensory nerve inactivation. *J Musculoskelet Neuronal Interact*. 2014; 14:1–9. [PubMed: 24583535]
- Hill EL, Elde R. Distribution of CGRP-, VIP-, D beta H-, SP-, and NPY-immunoreactive nerves in the periosteum of the rat. *Cell Tissue Res*. 1991; 264:469–480. [PubMed: 1714353]
- Hosmane S, Tegenge MA, Rajbhandari L, Uapinyoying P, Kumar NG, Thakor N, Venkatesan A. Toll/interleukin-1 receptor domain-containing adapter inducing interferon-beta mediates microglial phagocytosis of degenerating axons. *J Neurosci*. 2012; 32:7745–7757. [PubMed: 22649252]
- Howe CL, Mobley WC. Long-distance retrograde neurotrophic signaling. *Current opinion in neurobiology*. 2005; 15:40–48. [PubMed: 15721743]
- Howe CL, Valletta JS, Rusnak AS, Mobley WC. NGF signaling from clathrin-coated vesicles: evidence that signaling endosomes serve as a platform for the Ras-MAPK pathway. *Neuron*. 2001; 32:801–814. [PubMed: 11738027]
- Huang EJ, Reichardt LF. Trk receptors: roles in neuronal signal transduction. *Annual review of biochemistry*. 2003; 72:609–642.
- Hukkanen M, Konttinen YT, Rees RG, Gibson SJ, Santavirta S, Polak JM. Innervation of bone from healthy and arthritic rats by substance P and calcitonin gene related peptide containing sensory fibers. *The Journal of rheumatology*. 1992; 19:1252–1259. [PubMed: 1383542]
- Ibrahim AI, Hawamdeh ZM, Alsharif AA. Evaluation of bone mineral density in children with perinatal brachial plexus palsy: effectiveness of weight bearing and traditional exercises. *Bone*. 2011; 49:499–505. [PubMed: 21640214]
- Indo Y, Tsuruta M, Hayashida Y, Karim MA, Ohta K, Kawano T, Mitsubuchi H, Tonoki H, Awaya Y, Matsuda I. Mutations in the TRKA/NGF receptor gene in patients with congenital insensitivity to pain with anhidrosis. *Nature genetics*. 1996; 13:485–488. [PubMed: 8696348]
- Jackson MZ, Gruner KA, Qin C, Tourtellotte WG. A neuron autonomous role for the familial dysautonomia gene ELP1 in sympathetic and sensory target tissue innervation. *Development*. 2014; 141:2452–2461. [PubMed: 24917501]
- Jimenez-Andrade JM, Mantyh WG, Bloom AP, Xu H, Ferng AS, Dussor G, Vanderah TW, Mantyh PW. A phenotypically restricted set of primary afferent nerve fibers innervate the bone versus skin: therapeutic opportunity for treating skeletal pain. *Bone*. 2010; 46:306–313. [PubMed: 19766746]
- Kaplan DR, Stephens RM. Neurotrophin signal transduction by the Trk receptor. *Journal of neurobiology*. 1994; 25:1404–1417. [PubMed: 7852994]
- Kawaja MD, Smithson LJ, Elliott J, Trinh G, Crotty AM, Michalski B, Fahnestock M. Nerve growth factor promoter activity revealed in mice expressing enhanced green fluorescent protein. *The Journal of comparative neurology*. 2011; 519:2522–2545. [PubMed: 21456011]
- Ke MT, Imai T. Optical clearing of fixed brain samples using SeeDB. *Curr Protoc Neurosci*. 2014; 66 Unit 2 22.

- Kronenberg HM. Developmental regulation of the growth plate. *Nature*. 2003; 423:332–336. [PubMed: 12748651]
- Kugler JH, Tomlinson A, Wagstaff A, Ward SM. The role of cartilage canals in the formation of secondary centres of ossification. *J Anat*. 1979; 129:493–506. [PubMed: 541238]
- Kumar A, Brockes JP. Nerve dependence in tissue, organ, and appendage regeneration. *Trends in neurosciences*. 2012; 35:691–699. [PubMed: 22989534]
- Lentz SI, Knudson CM, Korsmeyer SJ, Snider WD. Neurotrophins support the development of diverse sensory axon morphologies. *J Neurosci*. 1999; 19:1038–1048. [PubMed: 9920667]
- Levi-Montalcini R, Angeletti PU. Nerve growth factor. *Physiol Rev*. 1968; 48:534–569. [PubMed: 4875350]
- Li C, Stanton JA, Robertson TM, Suttie JM, Sheard PW, Harris AJ, Clark DE. Nerve growth factor mRNA expression in the regenerating antler tip of red deer (*Cervus elaphus*). *PLoS One*. 2007; 2:e148. [PubMed: 17215957]
- Lutfi AM. Mode of growth, fate and functions of cartilage canals. *J Anat*. 1970; 106:135–145. [PubMed: 5413561]
- Mach DB, Rogers SD, Sabino MC, Luger NM, Schwei MJ, Pomonis JD, Keyser CP, Clohisy DR, Adams DJ, O'Leary P, et al. Origins of skeletal pain: sensory and sympathetic innervation of the mouse femur. *Neuroscience*. 2002; 113:155–166. [PubMed: 12123694]
- Madsen JE, Hukkanen M, Aune AK, Basran I, Moller JF, Polak JM, Nordsletten L. Fracture healing and callus innervation after peripheral nerve resection in rats. *Clin Orthop Relat Res*. 1998:230–240. [PubMed: 9646767]
- Maes C, Kobayashi T, Selig MK, Torrekens S, Roth SI, Mackem S, Carmeliet G, Kronenberg HM. Osteoblast precursors, but not mature osteoblasts, move into developing and fractured bones along with invading blood vessels. *Developmental cell*. 2010; 19:329–344. [PubMed: 20708594]
- Molliver DC, Snider WD. Nerve growth factor receptor TrkA is down-regulated during postnatal development by a subset of dorsal root ganglion neurons. *The Journal of comparative neurology*. 1997; 381:428–438. [PubMed: 9136800]
- Moqrich A, Earley TJ, Watson J, Andahazy M, Backus C, Martin-Zanca D, Wright DE, Reichardt LF, Patapoutian A. Expressing TrkC from the TrkA locus causes a subset of dorsal root ganglia neurons to switch fate. *Nature neuroscience*. 2004; 7:812–818. [PubMed: 15247919]
- Mukoyama YS, Shin D, Britsch S, Taniguchi M, Anderson DJ. Sensory nerves determine the pattern of arterial differentiation and blood vessel branching in the skin. *Cell*. 2002; 109:693–705. [PubMed: 12086669]
- Muller M, Triaca V, Besusso D, Costanzi M, Horn JM, Koudelka J, Geibel M, Cestari V, Minichiello L. Loss of NGF-TrkA signaling from the CNS is not sufficient to induce cognitive impairments in young adult or intermediate-aged mice. *J Neurosci*. 2012; 32:14885–14898. [PubMed: 23100411]
- Nagano J, Tada K, Masatomi T, Horibe S. Arthropathy of the wrist in leprosy--what changes are caused by long-standing peripheral nerve palsy? *Archives of orthopaedic and trauma surgery*. 1989; 108:210–217. [PubMed: 2774872]
- Nakamura E, Nguyen MT, Mackem S. Kinetics of tamoxifen-regulated Cre activity in mice using a cartilage-specific CreER(T) to assay temporal activity windows along the proximodistal limb skeleton. *Dev Dyn*. 2006; 235:2603–2612. [PubMed: 16894608]
- Nakashima K, Zhou X, Kunkel G, Zhang Z, Deng JM, Behringer RR, de Crombrughe B. The novel zinc finger-containing transcription factor osterix is required for osteoblast differentiation and bone formation. *Cell*. 2002; 108:17–29. [PubMed: 11792318]
- Offley SC, Guo TZ, Wei T, Clark JD, Vogel H, Lindsey DP, Jacobs CR, Yao W, Lane NE, Kingery WS. Capsaicin-sensitive sensory neurons contribute to the maintenance of trabecular bone integrity. *J Bone Miner Res*. 2005; 20:257–267. [PubMed: 15647820]
- Olsen BR, Reginato AM, Wang W. Bone development. *Annual review of cell and developmental biology*. 2000; 16:191–220.
- Ono N, Ono W, Nagasawa T, Kronenberg HM. A subset of chondrogenic cells provides early mesenchymal progenitors in growing bones. *Nat Cell Biol*. 2014; 16:1157–1167. [PubMed: 25419849]

- Reichardt LF. Neurotrophin-regulated signalling pathways. *Philosophical transactions of the Royal Society of London Series B, Biological sciences*. 2006; 361:1545–1564. [PubMed: 16939974]
- Santavirta S, Kontinen YT, Nordstrom D, Makela A, Sorsa T, Hukkanen M, Rokkanen P. Immunologic studies of nonunited fractures. *Acta orthopaedica Scandinavica*. 1992; 63:579–586. [PubMed: 1471500]
- Schindelin J, Arganda-Carreras I, Frise E, Kaynig V, Longair M, Pietzsch T, Preibisch S, Rueden C, Saalfeld S, Schmid B, et al. Fiji: an open-source platform for biological-image analysis. *Nat Methods*. 2012; 9:676–682. [PubMed: 22743772]
- Scita G, Tenca P, Frittoli E, Tocchetti A, Innocenti M, Giardina G, Di Fiore PP. Signaling from Ras to Rac and beyond: not just a matter of GEFs. *Embo J*. 2000; 19:2393–2398. [PubMed: 10835338]
- Smeyne RJ, Klein R, Schnapp A, Long LK, Bryant S, Lewin A, Lira SA, Barbacid M. Severe sensory and sympathetic neuropathies in mice carrying a disrupted Trk/NGF receptor gene. *Nature*. 1994; 368:246–249. [PubMed: 8145823]
- Toscano E, della Casa R, Mardy S, Gaetaniello L, Sadile F, Indo Y, Pignata C, Andria G. Multisystem involvement in congenital insensitivity to pain with anhidrosis (CIPA), a nerve growth factor receptor (Trk A)-related disorder. *Neuropediatrics*. 2000; 31:39–41. [PubMed: 10774995]
- Wojtys EM, Beaman DN, Glover RA, Janda D. Innervation of the human knee joint by substance-P fibers. *Arthroscopy : the journal of arthroscopic & related surgery : official publication of the Arthroscopy Association of North America and the International Arthroscopy Association*. 1990; 6:254–263.
- Xing W, Cheng S, Wergedal J, Mohan S. Epiphyseal chondrocyte secondary ossification centers require thyroid hormone activation of Indian hedgehog and osterix signaling. *J Bone Miner Res*. 2014; 29:2262–2275. [PubMed: 24753031]
- Zhao H, Feng J, Seidel K, Shi S, Klein O, Sharpe P, Chai Y. Secretion of shh by a neurovascular bundle niche supports mesenchymal stem cell homeostasis in the adult mouse incisor. *Cell stem cell*. 2014; 14:160–173. [PubMed: 24506883]

HIGHLIGHTS

- TrkA sensory nerves extend from the DRG to sites of incipient bone formation
- Perichondrial osteochondral progenitors express NGF until early postnatal life
- Inhibiting NGF-TrkA signaling during embryogenesis impairs normal bone development
- NGF-TrkA signaling coordinates innervation, vascularization, and ossification

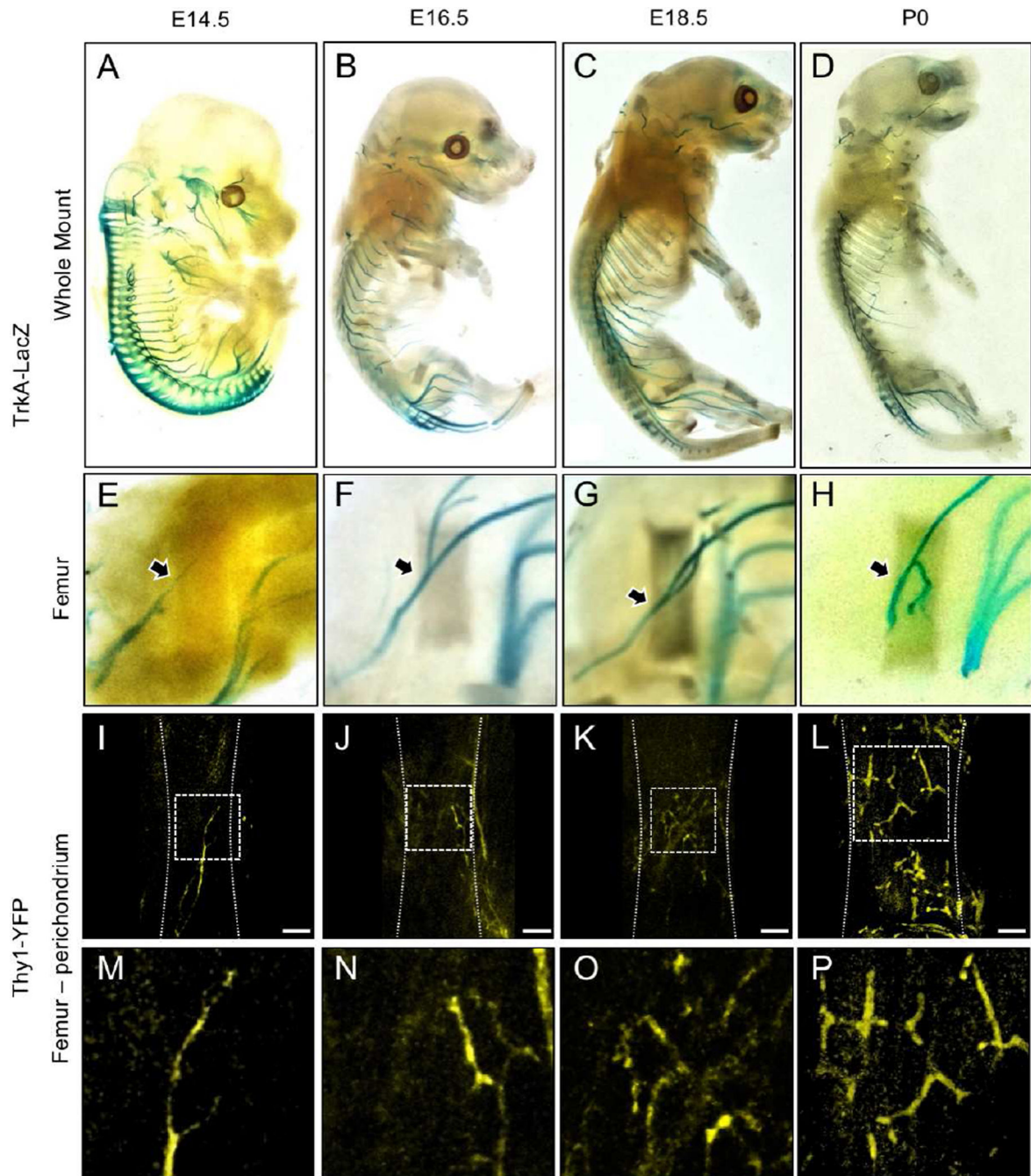


Figure 1. Innervation of the developing mouse hindlimb by TrkA sensory nerves

TrkA-LacZ embryos were subjected to X-Gal staining, then imaged intact at A) E14.5 B) E16.5 C) E18.5 and D) P0. Hindlimbs were then removed and imaged separately to illustrate the medial aspect of the femur at E) E14.5 F) E16.5 G) E18.5 and H) P0. Femurs from Thy1-YFP embryos were carefully stripped of soft tissue, optically cleared, then imaged by confocal microscopy at I) E14.5 J) E16.5 K) E18.5 and L) P0.5, with high powered insets (M–P) that show the progressive arborization of nerves on the surface of the bone. Arrows indicate TrkA-LacZ+ nerve axon at the perichondrial region. Scale bars are 100 microns.

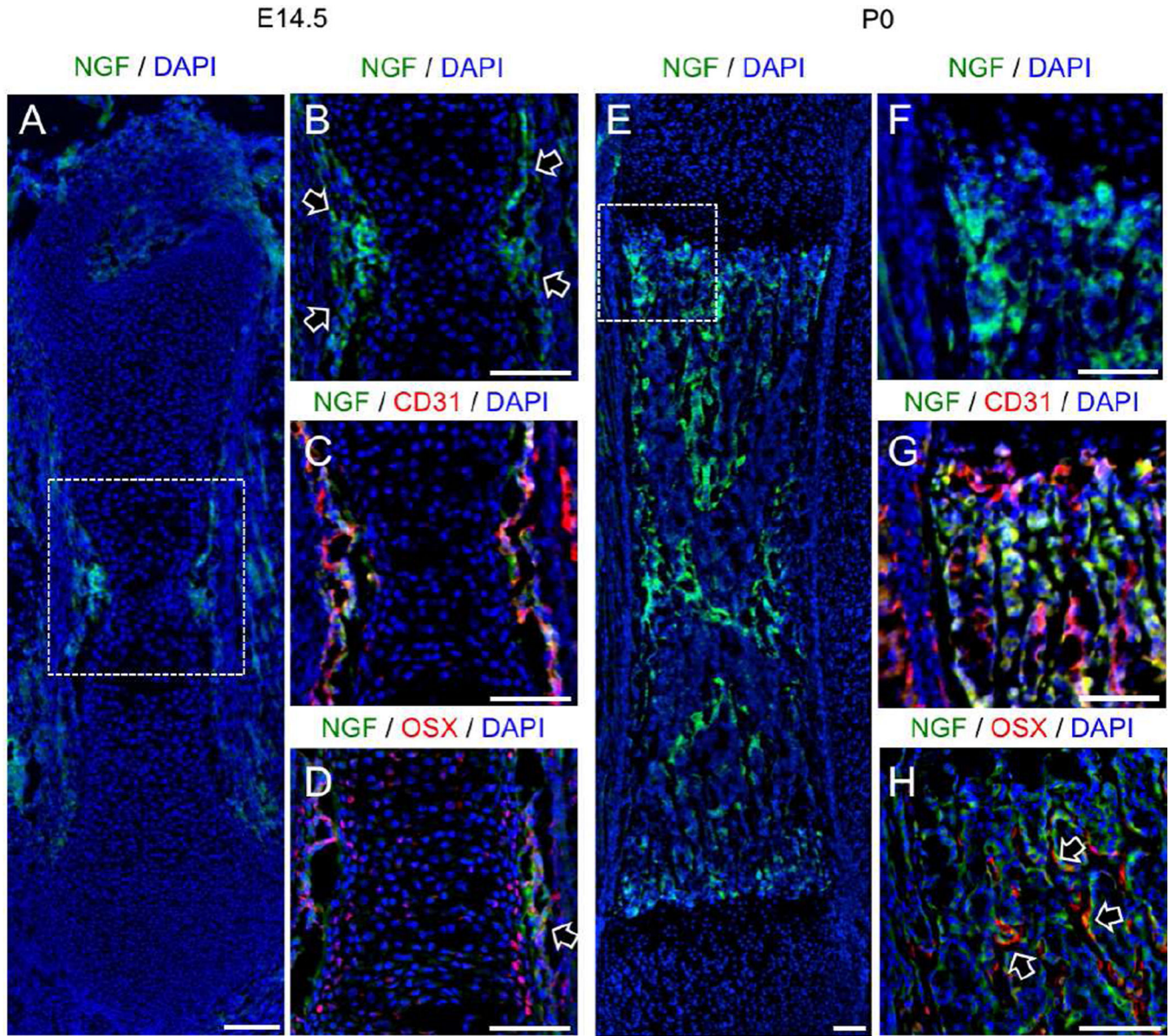


Figure 2. Localization of NGF expression in the developing mouse femur
 A) Femurs harvested from NGF-eGFP mice at E14.5 illustrate the expression of NGF at the perichondrial surface, with B) high powered inset showing NGF-expressing perichondrial cells (arrows) at the primary ossification center. C) Immunohistochemistry against CD31 illustrated that the primary ossification center is not yet vascularized. D) Immunohistochemistry against Osx marked some chondrocytes in the primary ossification center as well as perichondrial cells closely associated with NGF expression (arrow). E) Femurs harvested from NGF-eGFP mice at P0 illustrate the continued expression of NGF throughout the developing bone, with F) high powered inset at the growth plate. G) Immunohistochemistry against CD31 showed high vascularization but no correlation with NGF expression. H) Immunohistochemistry against Osx indicates close association of some

Osx-expressing cells with NGF expression (arrows). Scale bars are 100 microns. See also Figure S1, S2, and S3.

Author Manuscript

Author Manuscript

Author Manuscript

Author Manuscript

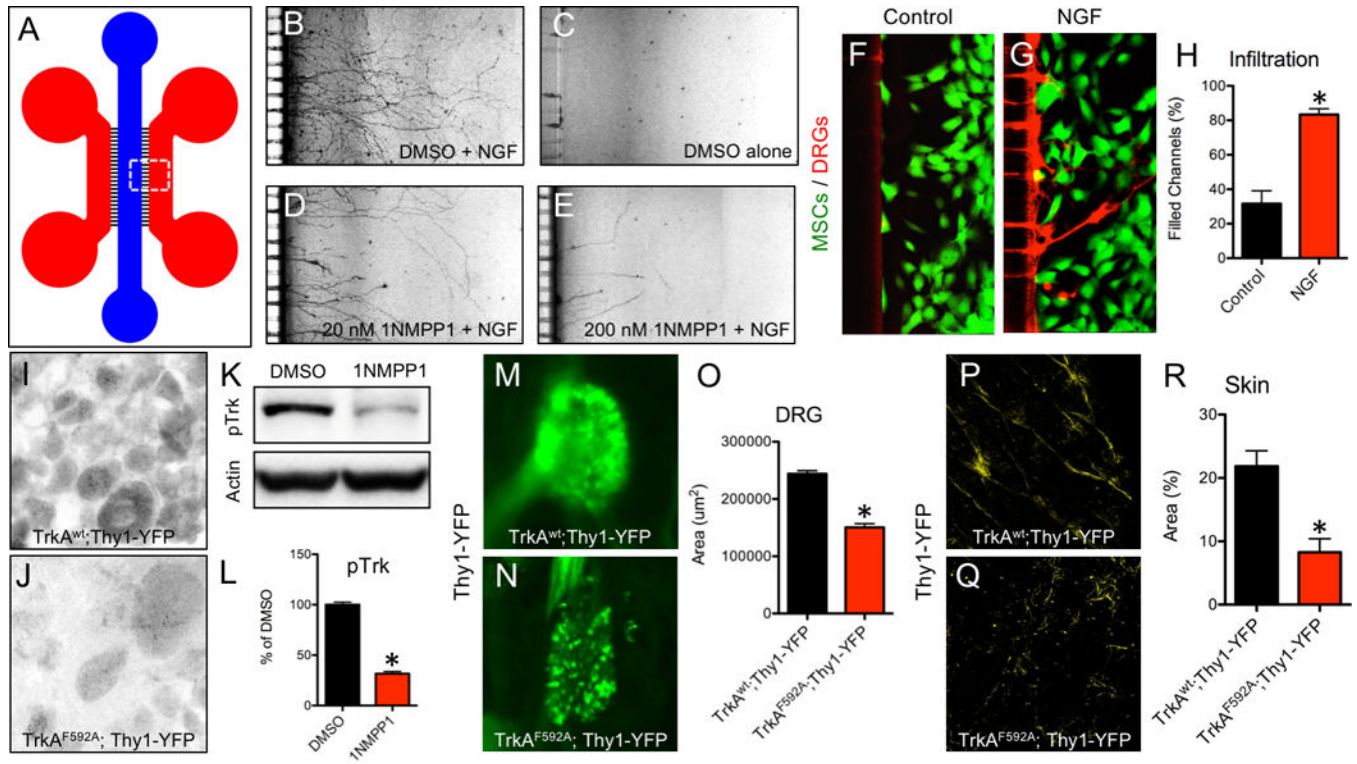


Figure 3. Inhibition of NGF-dependent TrkA signaling by 1NMPP1

A) A microfluidic device was used to culture DRG neurons plated in the blue compartment to project axons through microchannels ($3 \mu\text{m H} \times 10 \mu\text{m W}$) into the red compartment for visualization. Neuron outgrowth was visualized in B) Positive Control (DMSO + NGF), C) Negative Control (DMSO alone), D) Low Dose (20 nM 1NMPP1 + NGF), and E) High Dose (200 nM 1NMPP1 + NGF) cultures. MSCs were transfected with F) control or G) NGF cDNA and plated in the red compartment using media with suboptimal NGF, with H) axon infiltration quantification. DRGs were sectioned and stained with antibodies against pTrk in I) $\text{TrkA}^{\text{wt}}; \text{Thy1-YFP}$ and J) $\text{TrkA}^{\text{F592A}}; \text{Thy1-YFP}$ adult mice 24 hours after 1NMPP1 administration. K) Western blot against pTrk with loading control on protein extracted from DRGs of adult $\text{TrkA}^{\text{F592A}}; \text{Thy1-YFP}$ mice injected with DMSO or 1NMPP1 with L) quantification. Whole mount fluorescence imaging of intact DRGs at postnatal day 7 from M) $\text{TrkA}^{\text{wt}}; \text{Thy1-YFP}$ and N) $\text{TrkA}^{\text{F592A}}; \text{Thy1-YFP}$ littermates treated with 1NMPP1 during gestation with L) quantification. Whole mount fluorescence imaging of skin at postnatal day 7 from P) $\text{TrkA}^{\text{wt}}; \text{Thy1-YFP}$ and Q) $\text{TrkA}^{\text{F592A}}; \text{Thy1-YFP}$ littermates treated with 1NMPP1 during gestation with R) quantification. * $p < 0.05$ by unpaired Student's t-test.

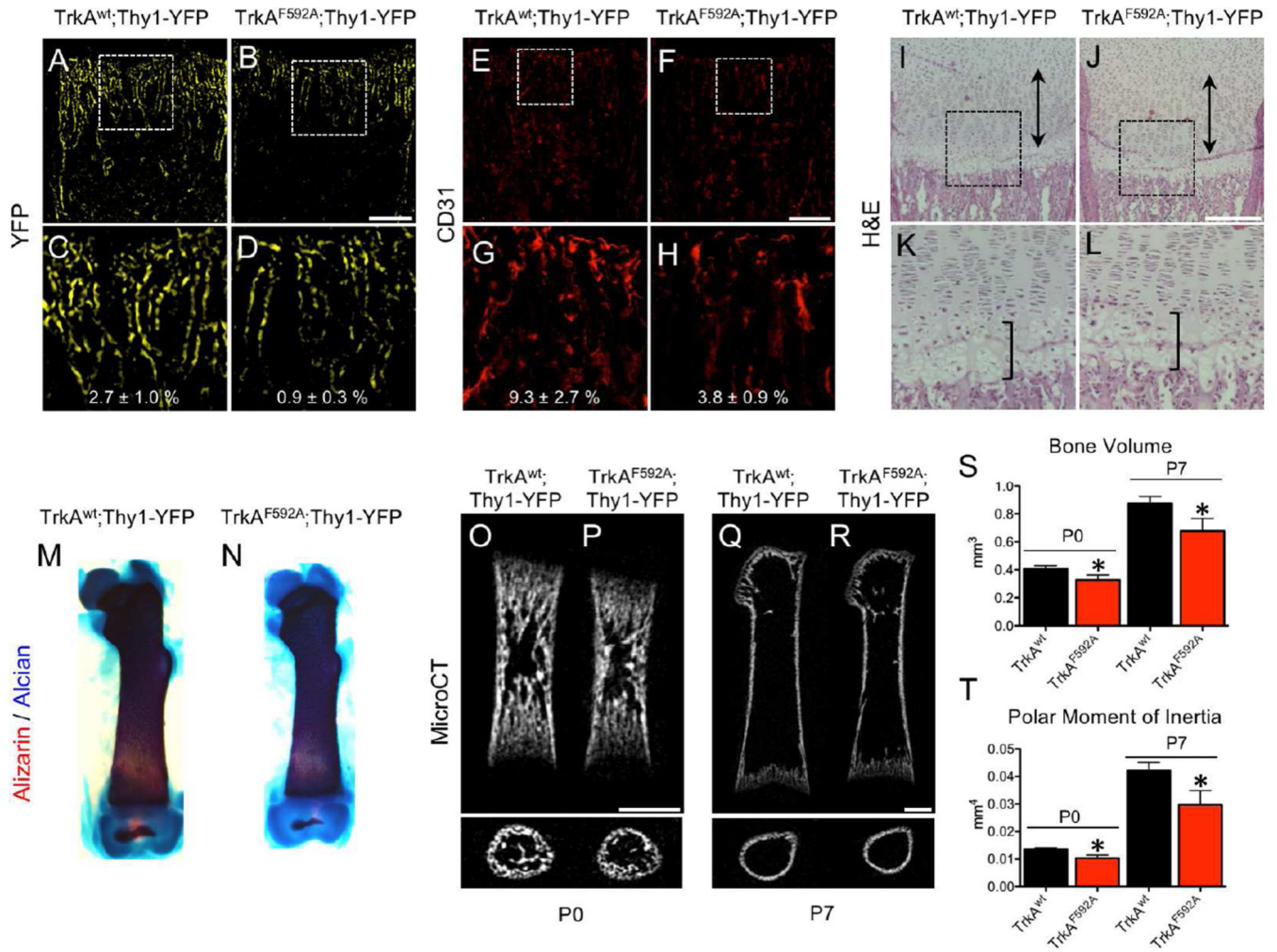


Figure 4. Inhibition of TrkA signaling impairs postnatal innervation, vascularization, and bone acquisition

Nerves were visualized at the femoral metaphysis by Thy1-YFP expression in frozen sections from A) TrkA^{wt};Thy1-YFP and B) TrkA^{F592A};Thy1-YFP mice at postnatal day 7, with high powered insets (C,D). Blood vessels were visualized at the femoral metaphysis by immunohistochemistry against CD31 in frozen sections from E) TrkA^{wt};Thy1-YFP and F) TrkA^{F592A};Thy1-YFP mice at postnatal day 7, with high powered insets (G,H). H&E staining of I) TrkA^{wt};Thy1-YFP and J) TrkA^{F592A};Thy1-YFP mice at postnatal day 7 with hypertrophic zone (bracket) and proliferative zone (double arrow) marked, with high powered insets (K,L). Skeletal preparations of M) TrkA^{wt};Thy1-YFP and N) TrkA^{F592A};Thy1-YFP femurs at postnatal day 7. MicroCT analysis of TrkA^{wt};Thy1-YFP and TrkA^{F592A};Thy1-YFP mice at postnatal day 0 (O,P) and day 7 (Q,R) with quantification of S) bone volume and T) polar moment of inertia. * $p < 0.05$ by unpaired Student's t-test. Scale bars are 100 microns. See also Figure S4, S5, and S7.

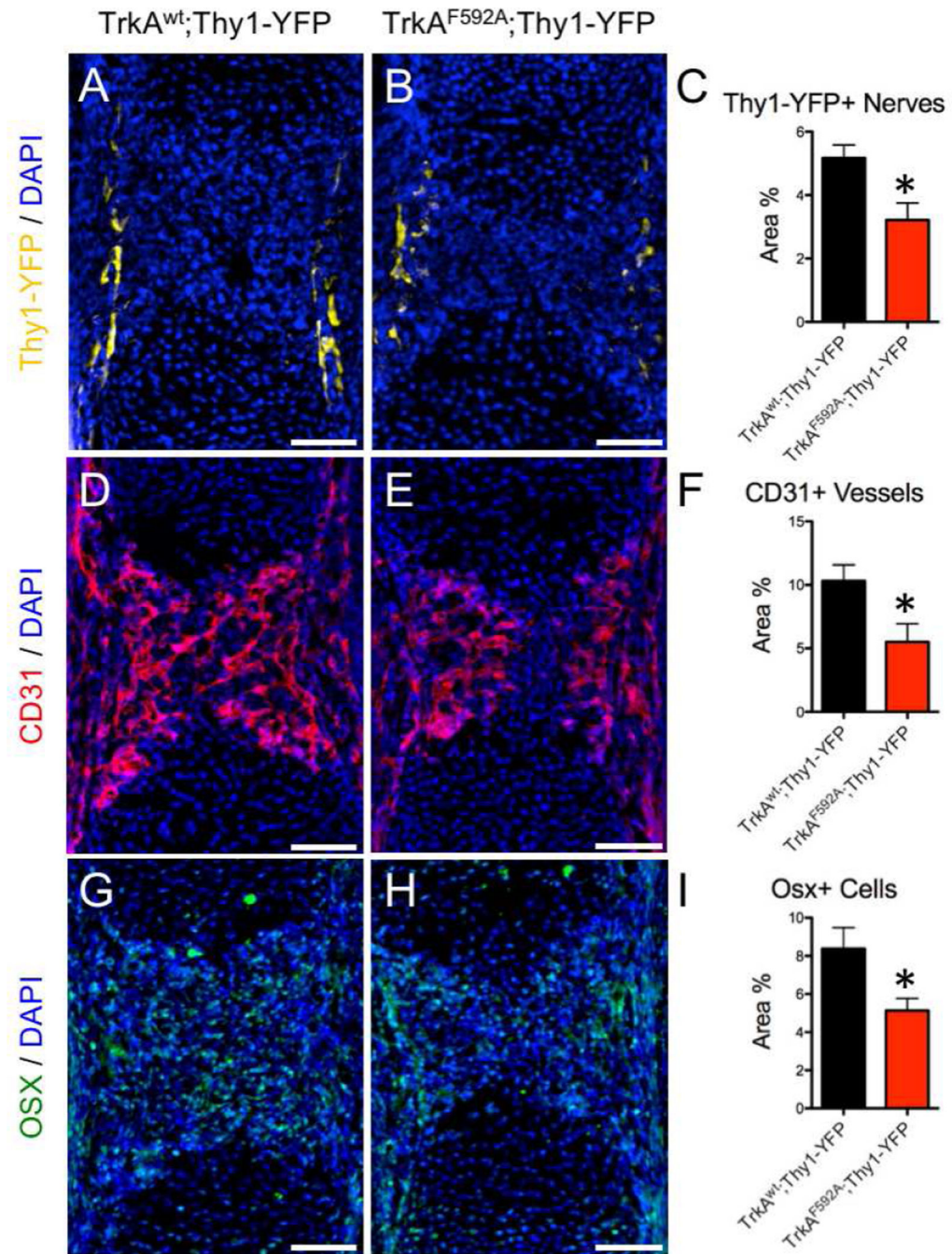


Figure 5. Inhibition of TrkA signaling impairs embryonic innervation, vascularization, and accumulation of osteoblast precursors

Frozen sections of the primary ossification center of the femur were analyzed for Thy1-YFP + nerves in A) TrkA^{wt};Thy1-YFP and B) TrkA^{F592A};Thy1-YFP mice at embryonic day 15.5 with C) quantification. Similarly, blood vessels were visualized by immunohistochemistry against CD31 in D) TrkA^{wt};Thy1-YFP and E) TrkA^{F592A};Thy1-YFP mice at embryonic day 15.5 with F) quantification. Finally, osteoprogenitor cells were analyzed by immunohistochemistry against Osterix (Osx) in G) TrkA^{wt};Thy1-YFP and H)

TrkA^{F592A};Thy1-YFP mice at embryonic day 15.5 with I) quantification. * $p < 0.05$ by Student's t-test. Scale bars are 100 microns.

Author Manuscript

Author Manuscript

Author Manuscript

Author Manuscript

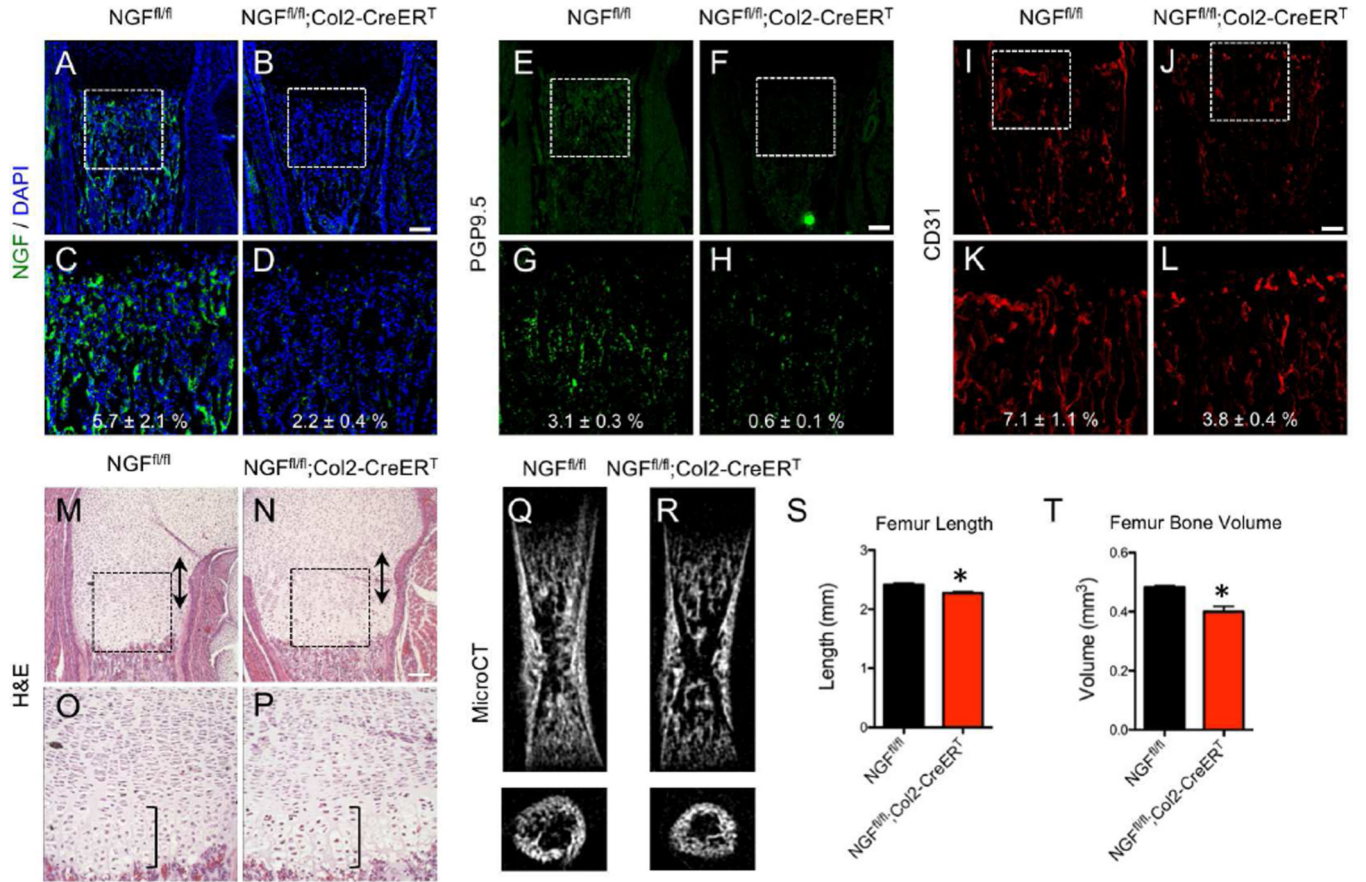


Figure 6. Disruption of NGF in osteochondral progenitors produces a skeletal phenotype similar to TrkA^{F592A} mice

Tamoxifen was administered to pregnant mothers at E11.5, and NGF^{fl/fl} and NGF^{fl/fl};Col2-CreER^T offspring were harvested for analysis at postnatal day 0. Expression of NGF was visualized at the femoral metaphysis by immunohistochemistry against NGF on frozen sections from A) NGF^{fl/fl} and B) NGF^{fl/fl};Col2-CreER^T mice, with high powered insets (C,D). Nerves were visualized at the femoral metaphysis by immunohistochemistry against PGP9.5 on frozen sections from E) NGF^{fl/fl} and F) NGF^{fl/fl};Col2-CreER^T mice, with high powered insets (G,H). Blood vessels were visualized at the femoral metaphysis by immunohistochemistry against CD31 on frozen sections from I) NGF^{fl/fl} and J) NGF^{fl/fl};Col2-CreER^T, with high powered insets (K,L). H&E staining of paraffin sections of femurs from M) NGF^{fl/fl} and N) NGF^{fl/fl};Col2-CreER^T mice with hypertrophic zone (bracket) and proliferative zone (double arrow) marked, with high powered insets (O,P). MicroCT analysis of Q) NGF^{fl/fl} and R) NGF^{fl/fl};Col2-CreER^T with quantification of S) femur length and T) femur bone volume. * p < 0.05 by unpaired Student's t-test. Scale bars are 100 microns. See also Figure S6 and S7.

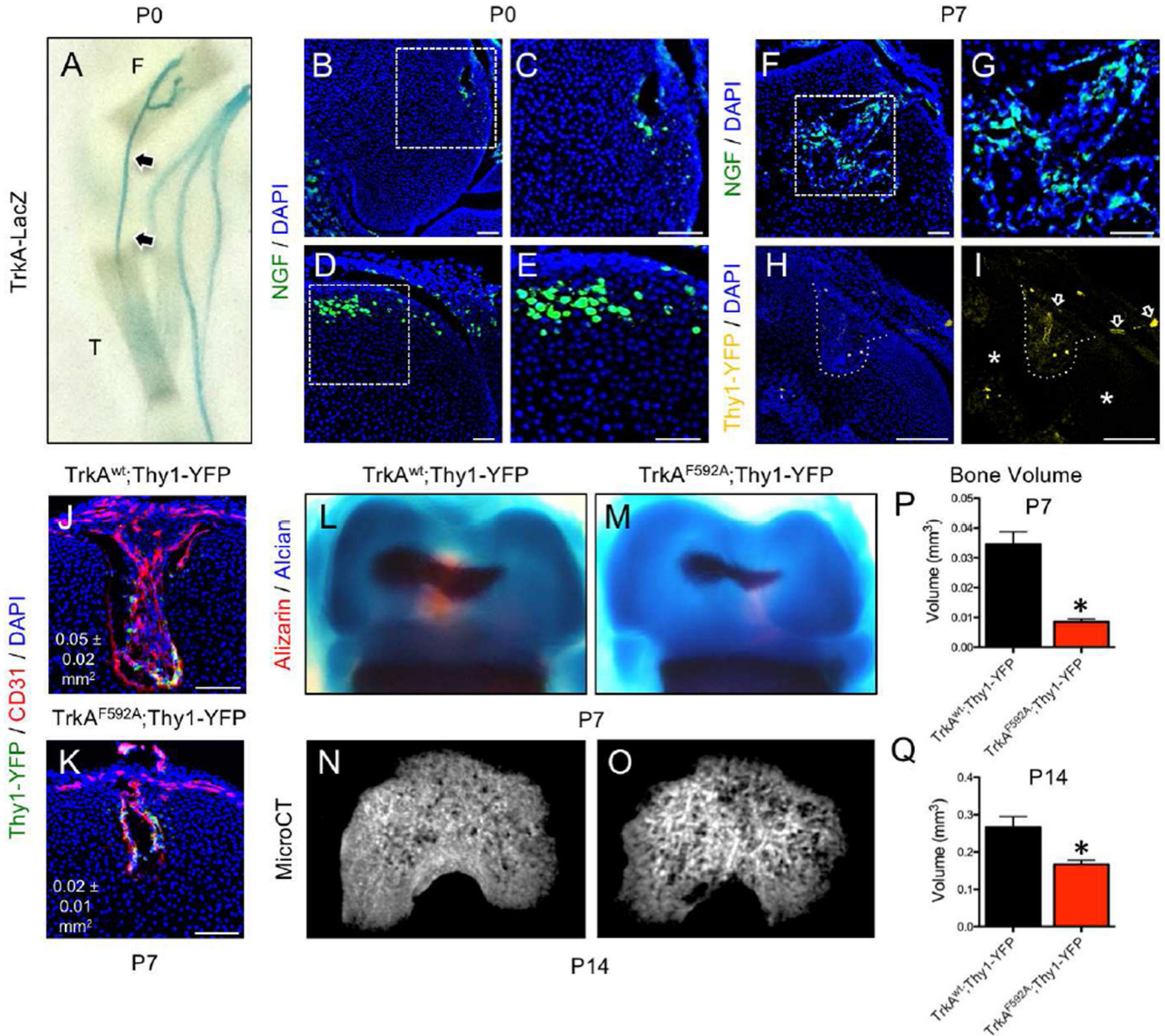


Figure 7. Inhibition of TrkA signaling impairs secondary ossification

A) Whole mount images of TrkA-LacZ mice subjected to X-Gal staining at postnatal day 0 illustrate TrkA sensory nerve axons terminating at primary ossification centers and accessible to secondary ossification centers (arrows), with T (tibia) and F (femur) labeled. **B)** NGF expressing cells were observed at the leading front of nascent vascular canals in femurs from NGF-eGFP mice at postnatal day 0, with **C)** high powered inset. **D)** NGF expressing cells were also found at positions of putative canal formation in femurs from NGF-eGFP mice at postnatal day 0, with **E)** high powered inset. **F)** By postnatal day 7, the marrow of the secondary ossification centers had abundant NGF expressing cells, with **G)** high powered inset. **H)** In TrkA^{wt};Thy1-YFP mice analyzed at postnatal day 7, Thy1-YFP⁺ nerves were found within the vascular canal (dotted line). **I)** These Thy1-YFP⁺ nerves had infiltrated the canal from the perichondrial region (arrows), whereas nerves were not observed in non-

vascularized regions of the epiphysis (asterisks). 1NMPP1 (40 μ M) was administered to pregnant heterozygous $\text{TrkA}^{\text{F592A/wt}}$ mice and pups were sacrificed at postnatal days 7 and 14. J) At postnatal day 7, $\text{TrkA}^{\text{wt}};\text{Thy1-YFP}$ mice had larger and more vascularized secondary ossification canals at the distal femur than K) $\text{TrkA}^{\text{F592A}};\text{Thy1-YFP}$ mice. L) $\text{TrkA}^{\text{wt}};\text{Thy1-YFP}$ mice had a significantly larger secondary ossification center in the distal femur than M) $\text{TrkA}^{\text{F592A}};\text{Thy1-YFP}$ by skeletal preparation at postnatal day 7. N) Similarly, microCT reconstruction revealed that $\text{TrkA}^{\text{wt}};\text{Thy1-YFP}$ mice had significantly increased bone volume than O) $\text{TrkA}^{\text{F592A}};\text{Thy1-YFP}$ at postnatal day 14. Quantification of bone volume by microCT was performed at both P) P7 and Q) P14. * $p < 0.05$ by Student's t-test. Scale bars are 100 microns.